Investigation into the Effect of Thickness on Three- and Four-point Single Edge Notch Bend Specimens Using Two- and Three-dimensional Elastic–Plastic Stress Analyses

R. W. J. KOERS*, H. BRAAM** and A. BAKKER***

*Koninklijke/Shell-Laboratorium, Amsterdam (Shell Research B.V.), P.O. Box 3003, 1003 AA Amsterdam, The Netherlands

**Netherlands Energy Research Foundation (ECN), P.O. Box 1, 1755 ZG Pettern, The Netherlands

***Delft University of Technology, P.O. Box 5025, 2600 GA Delft, The Netherlands

ABSTRACT

The effect of thickness in fracture behaviour has been investigated experimentally and through elastic-plastic finite element analyses on three- and four-point Single Edge Notch Bend specimens. Special attention was paid to the constraint at the crack tip, the distribution of the J-integral and the Crack Tip Opening Displacement along the crack front. The results of experiments and of the stress analyses revealed there is an upper limit to the size of the transition zone, in which the stress state along the crack front develops from plane stress at the free surface to a triaxial stress state with high constraint deeper in the specimen. This upper limit appears to be 6 mm for the thicknesses above 30 mm for a Fe 510 Nb steel at −70 °C.

KEYWORDS

Effect of thickness, Single Edge Notch Bend specimens, Finite element, Crack Tip Opening Displacement (CTOD), J-integral, Fe 510 Nb

INTRODUCTION

The thickness effect on fracture toughness mainly consists of the following two components. One is based on the statistical distribution of zones of low toughness in material and the other is related to the stress state in the vicinity of the crack front (constraint at the crack front). Due to stress concentration near the crack tip, the material near the crack tip tends to contract perpendicularly to the major stress axis of loaded cracked structures. However, the material is restrained by surrounding material due to compatibility requirements. The restraint produces a triaxial stress state, which increases the maximum principal stress at which yielding occurs.

To investigate the effect of thickness in fracture behaviour, we conducted both experiments and two- and three-dimensional elastic-plastic finite element (FE) analyses on three- and four-point Single Edge Notch Bend

specimens (3SENB and 4SENB). The experimental results for comparison with the FE results are reported by Van Rongen (1987). The thicknesses analysed were B=30, 70 and 110 mm for the 4SENB specimen and B=30 mm for the 3SENB specimen. The suitability of various global and local crack tip constraint parameters was investigated for prediction of the observed thickness effect.

MATERIAL, GEOMETRY AND FINITE ELEMENT ANALYSIS

Both two-dimensional and three dimensional FE analyses were carried out on 3SENB and 4SENB specimens. The geometry and dimensions of the analysed specimens are given in Figure 1. Because of symmetry only one quarter of the specimens needed to be modelled.

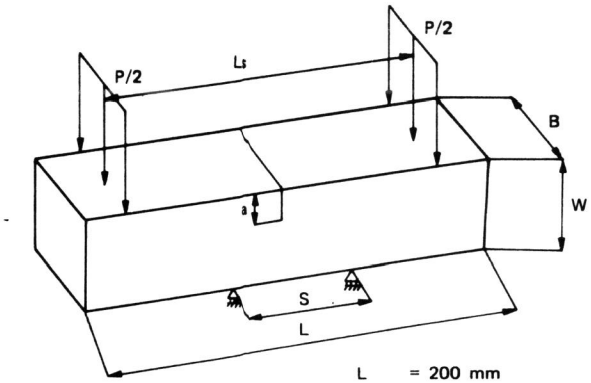

S = 0 mm (SENB3)
60 mm (SENB4)
B = 30 mm (SENB3)
30, 70 and 110 mm (SENB4)
L = 200 mm
W = 30 mm
a/W = 0.3
Ls = 120 mm (SENB3)
180 mm (SENB4)

Fig. 1. Geometry and dimensions of the analysed specimens

For all cases, the half thickness was modelled by three layers of elements; for the 4SENB specimen with B=30 mm an additional analysis was performed with five element layers over the half thickness to prove convergence. For the latter case the FE mesh is given in Figure 2.

The layer thicknesses are given in Table 1. Convergence of the two-dimensional FE analysis was proved by carrying out analyses for several mesh refinements of the overall mesh and size of the collapsed elements around the crack tip, and by investigating the effect of the load step size and convergence criterion. Finally in all the analyses the load was applied by prescribing the load line displacement in equal steps of 0.1 mm.

In the three-dimensional case the overall mesh was modelled using 20-node quadratic isoparametric brick elements with a 3 x 3 x 3 Gauss integration scheme. Around the crack tip, these elements were collapsed to produce a 1/r strain singularity around the crack tip, which is characteristic of a loaded crack in the case of an elastic-perfectly-plastic material (Koers, 1988).

Table 1. Layer thickness of the FE mesh

Thickness (mm)	Layer (mm)					Specimen type analysed	
	I	II	III	IV	V	3SENB	4SENB
30	0.5	1.0	1.5	3.0	9.0	–	x
30	1.1	3.5	10.4			x	x
70	4.6	10.4	20.0			–	x
110	4.6	15.4	35.0			–	x

← Free surface Mid-plane →

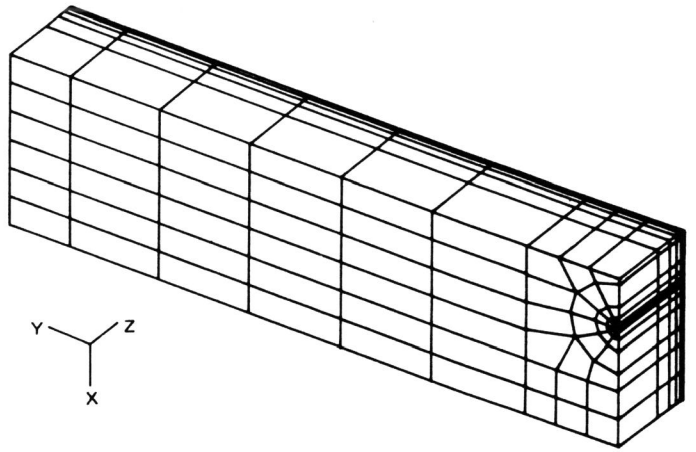

Fig. 2. Finite element mesh for B=30 mm with 5 element layers

Standard and collapsed 8-node quadratic isoparametic plate elements with a 3 x 3 Gauss integration scheme were used for the plane strain and plane stress analyses. For the FE analyses, the general-purpose FE program MARC (MARC) was used with the following program options:

- Newton Raphson (tangent stiffness) numerical iteration procedure;
- Small strain theory;
- Incremental flow theory of plasticity with isotropic hardening.

The engineering stess-strain curve used in the analyses of the tested material (Fe 510 Nb) at -70 ^{o}C, is given in Figure 3 (van Rongen, 1987). Young's modulus and Poisson's ratio are taken to be E = 215 GPa and ν = 0.28.

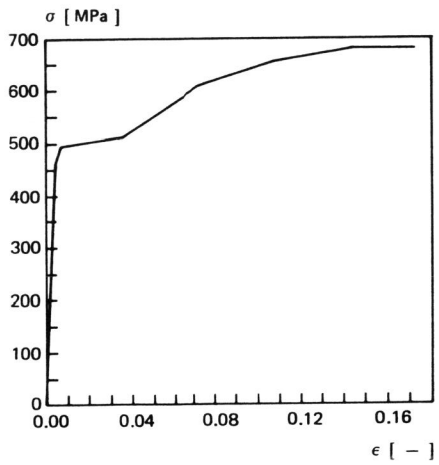

Fig. 3. Engineering stress-strain curve, Fe 510 Nb, at −70 °C

J-INTEGRAL

Because of a number of numerical difficulties in calculating the J contour integral[1], the calculation in a three-dimensional cracked body is not commonly based on the contour integral but on the concept of energy released by a virtual crack extension (VCE). The VCE method was originally developed by Hellen (1979) and (independently) by Parks (1974,1978) and was strongly linked to the finite element description of the structure. Subsequently, deLorenzi (1982) derived an alternative VCE formulation using an analytical approach. A detailed description and comparison of both the contour integral and the VCE method is given by Bakker (1984). In the analyses both the VCE method of Parks and the one of deLorenzi were used.

THE CRACK TIP OPENING DISPLACEMENT (CTOD)

For the 3SENB geometry, the definition of Figure 4 has been compared with the definition of the British Standard 5762:1979 (BSI, 1979) The expression of CTOD, δ, in accordance with the BSI definition is given by:

$$\delta_{BSI} = \frac{K^2(1-\nu^2)}{2\sigma_Y E} + \frac{0.4(W-a)V_p}{0.4W + 0.6a + z} \quad \text{with } K = \frac{YP}{B\sqrt{W}} \qquad (1)$$

where P is the applied load, V_p the plastic component of the clip gauge opening displacement, Y = 6.07 for a/W = 0.3, W the specimen width, B the specimen thickness, a the crack length and z the distance of the clip gauge location from the test specimen surface. In our analysis z = 0.

[1] Note that the term contour integral originates from two-dimensional applications, but that it is intended to cover both two- and three-dimensional applications here.

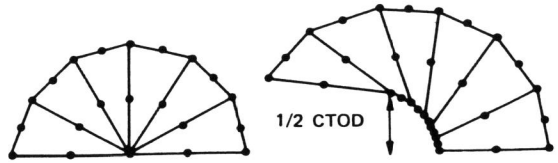

Fig. 4. Deformation of the crack tip, and definition of CTOD

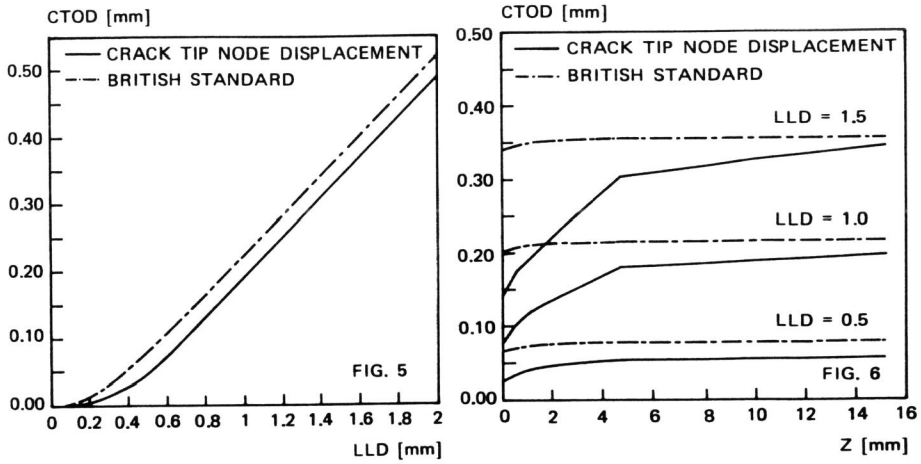

Fig. 5. Two-dimensional comparison of CTOD definitions, 3SENB specimen

Fig. 6. Three-dimensional comparison of CTOD definitions, 3SENB specimen

A comparison of the CTOD calculated according to equation (1) and that of Figure 4 is given in Figures 5 and 6 for the two- and three-dimensional analysis, respectively. The definition of Figure 4 has been used in the subsequent analyses.

RESULTS

Load versus Load-Line-Displacement

The calculated load per unit thickness versus the load-line-displacement (LLD) curves are presented in Figures 7 and 8 for the 4SENB and 3SENB specimens, respectively. Besides the 3-D solutions, the plane strain and plane stress solutions are also given. As could be expected, the behaviour of the specimens becomes stiffer with increasing thickness. The analysis on the 30 mm thick 4SENB specimen, with five element layers over the half thickness, proved convergence of the analysis with three layers of elements. The difference in load was less than 0.4 %.

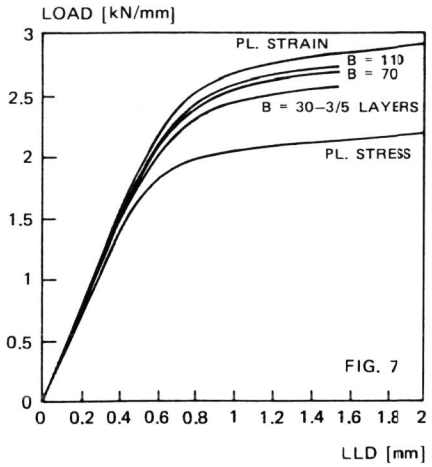

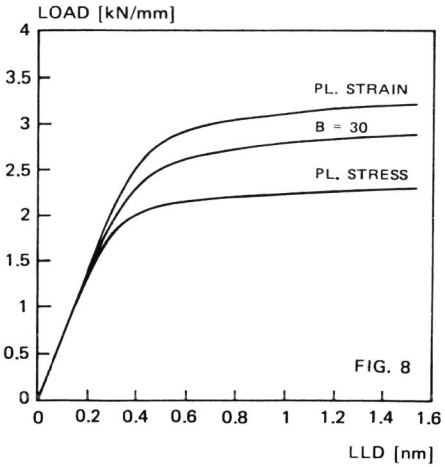

Fig. 7. Load versus load-line-displacement, 4SENB specimen

Fig. 8. Load versus load-line-displacement, 3SENB specimen

J-integral

In Figure 9 the J distribution of the 4SENB specimens along the crack front is presented for LLD = 0.5, 1.0 and 1.5 mm. From this figure it appears that at each load level the curves for B = 30, 70 and 110 mm almost coincide. This means that the J distribution for a 4SENB specimen with thickness between 30 mm and 110 mm can be derived from this figure. The thickness of the transition zone from the free surface, where a state of plane stress exists, to the central region, where a high triaxial stress exists with an upper limit of constraint, does not depend on the thickness of the specimen for B ≥ 30 mm.

It was observed that the shape of the fatigue crack front was similar to the J versus distance from the free surface graphs in that the crack growth, retarded at the specimen surface, reached a peak Z mm from the free surface and then gradually decreased towards the specimen mid-thickness, see Figure 10. The average values of Z were 5.9 mm for B = 30 mm and 6.5 mm for B = 70 and 110 mm. Note that at −70 °C the specimens with thickness B = 30 mm failed by cleavage after some stable ductile crack growth, whilst for both B = 70 and 110 mm they failed directly by cleavage.

The tested specimens were fatigue pre-cracked. When we assume that fatigue crack growth is controlled by the absolute value (K) and fluctuation (ΔK) of the stress intensity factor, the shape of the crack front is determined by K. Therefore, it is reasonable to compare the shape of the crack front with the distribution of J for small LLD. Although crack front curvature not has been modelled, the agreement between the calculated transition zone and Z is very good. For the 3SENB specimen the same tendencies of the J distribution along the crack front were found.

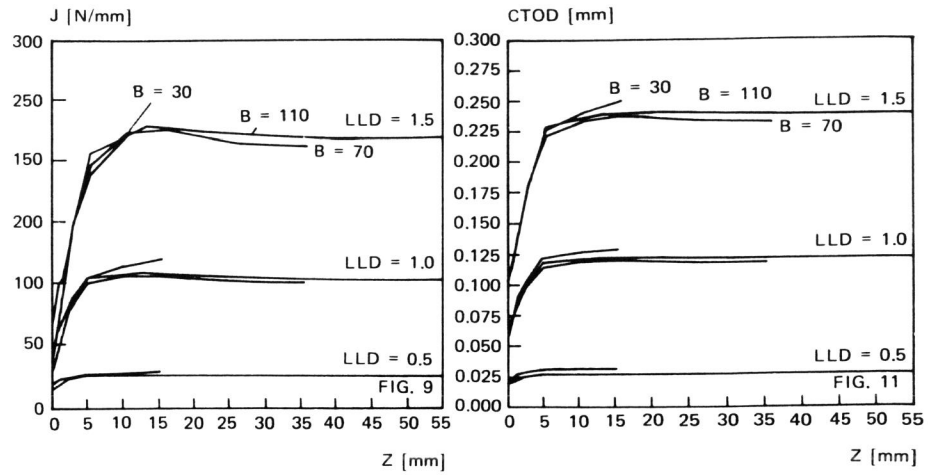

Fig. 9. J distribution along the crack front for three load levels, 4SENB specimen

Fig. 11. CTOD distribution along the crack front for three load levels, 4SENB specimen

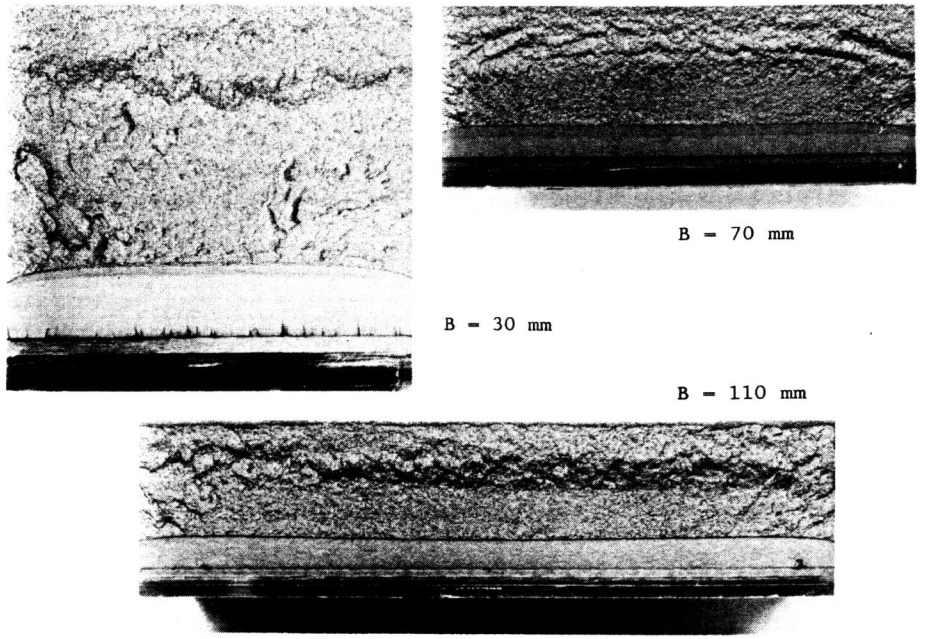

Fig. 10. Crack front for B = 30, 70 and 110 mm, 4SENB specimen

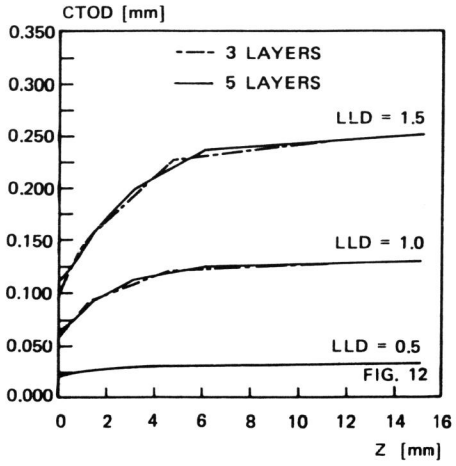

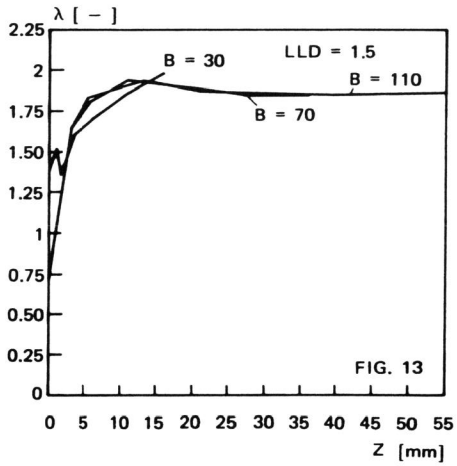

Fig. 12. CTOD distribution along the crack front for 4SENB specimen, B = 30 mm, three and five- element layers

Fig. 13. Distribution of λ along the crack front, LLD = 1,5 mm, 4SENB specimen

Crack Tip Opening Displacement (CTOD)

The distributions of CTOD along the crack front for the 4SENB specimens are presented in Figure 11 for LLD = 0.5, 1.0 and 1.5 mm. The trends found for J were as expected to exist for the CTOD. The convergence of the FE mesh is demonstrated by the good agreement of the CTOD results for B = 30 mm with 3 and 5 layers of elements (see Figure 12).

CONSTRAINT PARAMETERS

Both J and δ are considered to be global fracture-characterizing parameters. Since both parameters characterize the same phenomenon, there exists between them a relation that is usually written in the following linear form:

$$J = \lambda \sigma_Y \delta \qquad (2)$$

where λ is a constant depending on the geometric condition of plane strain or plane stress and the strain hardening of a material [10]. Since the specimen thickness and the loading condition are the only variations in our analyses, λ is considered to be a parameter which might prescribe constraint as a function of specimen thickness and loading condition. For the 4SENB specimens with B = 30, 70 and 110 mm, the distribution of λ along the crack front has been plotted in Figure 13 for LLD = 1.5 mm.

Alternative constraint parameters can be calculated from the stresses and strains locally around the crack tip. Here two parameters will be con-

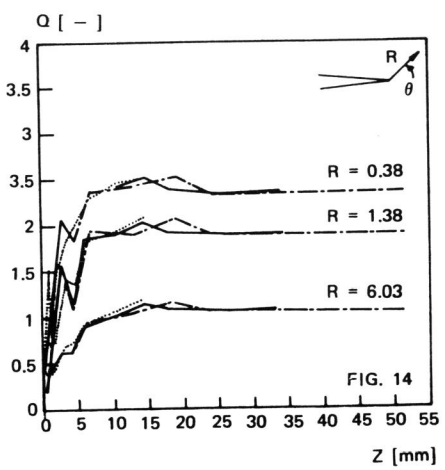

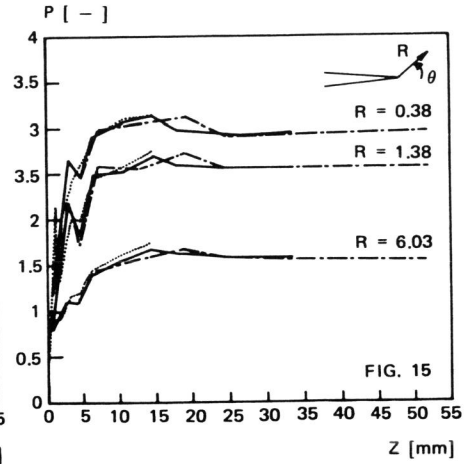

Fig. 14. Distribution of q along the crack front, LLD = 1.5 mm, 4SENB specimen

Fig. 15. Distribution of p along the crack front, LLD = 1.5 mm, 4SENB specimen

sidered. The first parameter calculated from the stresses was the ratio of the mean (hydrostatic) stress, σ_m, to the von Mises stress, σ_{eq}:

$$q = \sigma_m / \sigma_{eq} \qquad (3)$$

This parameter has been calculated because it has been shown that q contributes to the void growth rate [11]. The distribution of q near the ligament ($\theta = 15^o$ and R = 0.38, 1.38 and 6.03 mm) for the 4SENB specimens are given in Figure 14, LLD = 1.5 mm. The same tendencies were found for the 3SENB specimen.

The second stress-related parameter calculated was the ratio of the maximum principal stress, σ_1, to the von Mises stress:

$$p = \sigma_1 / \sigma_{eq} \qquad (4)$$

This parameter has been calculated because σ_1 should be taken into account for cleavage fracture. The distribution of p near the ligament is given in Figure 15, LLD = 1.5 mm. It can be observed that both p and q have in the same way and the results of the thinner specimens B = 30 and 70 mm coincide with that of B = 110 mm, corresponding the CTOD, J and λ results. The p and q results show a large fluctuation near the free surface.

This fluctuation originates from numerical procedures used to calculate the stress components in spite of the fact that the von Mises yield criterion was met. The equivalent von Mises stress curves are given in Figure 16. Although this yield criterion was met each stress component gave fluctuations as seen in Figures 14 and 15.

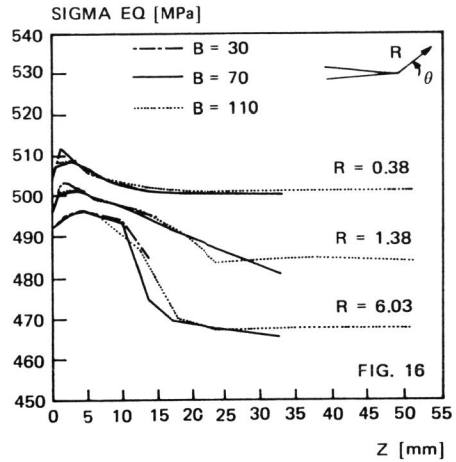

Fig. 16. Von Mises stress distribution along the crack front, LLD = 1.5 mm, 4SENB specimen

DISCUSSION

Near the free surface of a through-thickness crack, where a plane stress state exists, J and CTOD are low. In the centre a plateau value of J and CTOD are reached, provided that the thickness is sufficiently large ($B > 2\alpha_{tz}$) to develop a triaxial stress state with sufficient constraint. The width α_{tz} of the transition zone, where J and CTOD increase to the plateau value, is independent of thickness for the material studied. It is expected, though, that α_{tz} increases with plasticity at the crack tip, i.e. with decreasing strain hardening and with decreasing constraint.

Three different constraint parameters calculated to characterize the triaxiality of the stress state at the crack tip (ratio of maximum principal stress to von Mises stress, ratio of hydrostatic stress to von Mises stress, and ratio of J to the product of CTOD and yield stress) show the same qualitative behaviour along the crack front.

No significant differences were found between the J, CTOD and constraint parameters calculated for the 3SENB and 4SENB specimens. It was observed from the experimental results, however, that the 4SENB specimens failed earlier by cleavage than the 3SENB specimens.

From the load versus LLD curves it follows that for the thicker specimens the whole specimen behaves as if it is in a plane strain condition. For the thinner specimens the global behaviour is plane stress and the area with high constraint is concentrated at the crack tip region near the mid-thickness.

In the analysis performed, the effect of thickness was investigated considering J, CTOD and different constraint parameters. Statistics-based models to explain scatter and the effect of thickness in measuring fracture toughness are given by Braam and Prij (1987), Slatcher (1986), Wallin and Törrönen (1986) and Ehl et al. (1986).

CONCLUSIONS

The observed decreasing fracture toughness with increasing thickness cannot be explained by the geometrical effect of thickness on the state of stress or other crack tip parameters. It may be explained, however, from the statistics of the micromechanics of unstable brittle fracture initiation.

For the material studied the size of the transition zone from the plane stress state at the specimen surface to a triaxial stress state with a high constraint, appears to be ≈ 6mm for $B \geq 30$ mm. This depth coincides remarkably closely with the distance from the free surface to the point where, for the specimens tested, the curved fatigue crack front changes to a straight line.

REFERENCES

Bakker, A. (1984). The Three-dimensional J-integral – An Investigation into its Use for Post-Yield Fracture Safety Assessment, Doctoral Thesis, Delft University of Technology.

Braam, H. and J. Prij (1987). A Statistical Evaluation of the Thickness Effect of a SENB4 using the J-distribution along the Crack Front. Trans. of the 9th SMiRT, Vol. G, Lausanne, 17-21 August 1987.

British Standard Institution (1979). Methods for Crack Opening Displacement (COD) Testing, BS 5762:1979, UK.

DeLorenzi, H.G. (1982). On the Energy Release Rate and the J-integral for 3-D Crack Configuration, Int. J. Fracture, 19, 183-193.

Ehl, W., D. Munz and A. Brückner (1986). Scatter of Fracture Toughness in the Ductile-Brittle Transition, Proc. 6th Conf. on Fracture, ECF6, Amsterdam, June 15-20, 1986, 577-589.

Hellen, T.K. (1975). On the Method of Virtual Crack Extension. Int. J. Num. Methods in Eng., 9, 187-207.

Koers, R.W.J. (1988). Use of Modified Standard 20-Node Isoparametric Brick Elements for Representing Stress/Strain Fields at a Crack Tip for Elastic and perfectly Plastic Material. Int. J. Fracture, in the press.

MARC General Purpose Finite Element Analysis Program, version K2, MARC Analysis Research Corp. Palo Alto (California), U.S.A.

Parks, D.M. (1974). A Stiffness Derivative Finite Element Technique for Determination of Crack Tip Stress Intensity Factors. Int. J. Fracture, 10, 487-502.

Parks, D.M. (1978). Virtual Crack Extension: A General Finite Element Technique for J-integral Evaluation, Proc. 1st. Int. Conf. on Numerical Techniques in Fracture Mechanics, Swansea (Wales), 464-478.

Rice, J.R. and D.M. Tracey (1969). On the Ductile Enlargement of Voids in Triaxial Stress Fields. J. Mech. Phys. Solids, 17, 201-217.

Shih, C.F. (1981). Relationships between the J-integral and the Crack Opening Displacement for Stationary and Extending Cracks, J. Mech. Phys. Solids, 29, No. 4, 305-326.

Slatcher, S. (1986). The Probabilistic Modelling of Fracture Toughness. Proc. 6th Conf. on Fracture, ECF6, Amsterdam, June 15-20, 1986, 551-561.

Van Rongen, H.J.M. (1987). Final Report: First-Phase N.I.L. – Fracture Programme, BRE 87-09, NIL.

Wallin, K. and K. Törrönen (1986). Mechanism Based Statistical Requirements for Fracture Toughness Testing, Proc. 6th Conf. on Fracture, ECF6, Amsterdam, June 15-20, 1986, 563-575.